Molecular Spin-Flip Loss and a Dual Quadrupole Trap

David Reens,* Hao Wu, Tim Langen,† and Jun Ye
JILA, National Institute of Standards and Technology and the University of Colorado
Department of Physics, University of Colorado, Boulder, Colorado 80309-0440, USA
(Dated: May 1, 2017)

Doubly dipolar molecules exhibit complex internal spin-dynamics when electric and magnetic fields are both applied. Near magnetic trap minima, these spin-dynamics lead to enhancements in Majorana spin-flip transitions by many orders of magnitude relative to atoms, and are thus an important obstacle for progress in molecule trapping and cooling. The effect is strongest for Hund's case (a) states and is significant for Hund's case (b) as well. We study these internal spin-dynamics with OH molecules and devise a trap geometry where spin-flip loss can be tuned from over 200 s^{-1} to complete removal with only a weak external bias coil and with no sacrifice of trap strength.

The ultracold regime extends toward molecules on many fronts [1]. KRb molecules have reached lattice quantum degeneracy [2] and other bialkalis continue to progress [3, 4]. Creative and carefully engineered laser cooling strategies are tackling certain nearly vibrationally diagonal molecules [5–9]. A diverse array of alternative strategies have succeeded to greater or lesser extents on other molecules [10–15]. All of these molecules will require secondary strategies like evaporation or sympathetic cooling to make further gains in phase space density [25, 27**?**]. They also may face a familiar challenge: spin flip loss near the zero of a magnetic trap, but dramatically enhanced for many doubly dipolar molecules due to their internal spin dynamics in mixed electric and magnetic fields.

The knowledge of spin flips or Majorana hops as an eventual trap lifetime limit predates the very first magnetic trapping of neutrals [16]. Spin flips were directly observed near 50 μK and overcome with a time-orbiting potential trap [17] and a plugged dipole trap [18], famously enabling the first production of Bose-Einstein condensates. In our earlier investigations, we observed loss of magnetically trapped hydroxyl radicals (OH) with applied electric field [19]. This trap loss occurred for substates of OH's $X^2\Pi_{J=3/2}$ ground state manifold other than the doubly weak-field seeking one of positive parity and full spin polarization, the $|f, m_J = 3/2\rangle$ state, colored blue in Fig. 1. These other states eventually intersect levels of opposite parity at non-zero magnetic fields, where electric field can then open avoided crossings leading to trap loss. We now identify internal spin-dynamics leading to trap loss near zero magnetic field for the $|f, 3/2\rangle$ state that operates even in the 50 mK range and below.

These internal spin-dynamics are subtle, having eluded three previous investigations of note: In [22] the analogues of atomic spin-flip loss for molecules in mixed fields were modeled, and a magnetic quadrupole trap for OH molecules with superposed electric field was specifically addressed. It was concluded that no significant loss enhancement due to electric field would be evident. This is true only for the approximate $^2\Pi_{1/2}$ Hamiltonian used

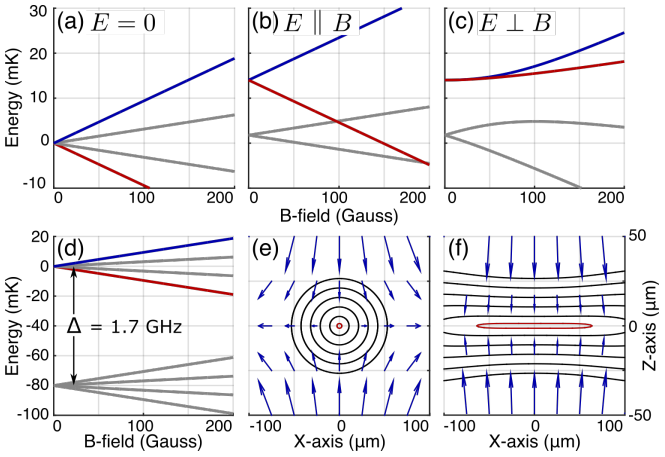

FIG. 1. Four Zeeman split lines in OH's $J = 3/2$ ground manifold are shown (a-c), with the trapped $|f, 3/2\rangle$ state in blue and its spin-flip partner $|f, -3/2\rangle$ in red. These states are shown with no E-field (a), with $E = 150$ V/cm and $E \parallel B$ (b), and with $E \perp B$ (c). Note the vastly reduced red-blue splitting in the latter case. The opposite parity manifold of electrically strong field seeking substates is split by the lambda doubling energy Δ (d). Energy splitting contours are shown every 2 mK near the zero of a magnetic quadrupole trap for OH molecules with 2 T/cm gradient [19] without E-field (e), and with $E = 150$ V/cm (f). The vectors give the quantization axis. Note the drastic widening of the lowest energy splitting contour.

in that study. In [21] E-fields were applied in our magnetic quadrupole trap to study E-field induced collisions. Although an initial approximation was made of the spin-dynamical effect, subsequent investigations have revealed it to be a threefold underestimate, enough to render deconvolution of any remaining collisional effect difficult. Finally, in [24] it was correctly noted that Hund's case (a) molecules maintain a quantization axis in mixed fields. The states of the molecule were shown to align with one of two quantization axes- either the vector sum or the vector difference of the dipole moment weighted fields $\mu_E\vec{E}$ and $\mu_B\vec{B}$. It was asserted that this would maintain quantization near the zero of a quadrupole trap and avoid spin-flip loss. As we now explain and demonstrate with

conclusive experimental evidence, quantization is indeed maintained, but spin-flip loss is enhanced.

Consider a magnetic quadrupole trap, where a weak-field seeking molecule remains trapped insofar as it adiabatically follows the field direction. Near the trap center, the direction changes most rapidly, causing loss. When electric field is added, it dominates in the trap center where the magnetic field is weakest. Quantization is maintained but the quantization axis does not rotate with the magnetic field. Further away from the trap center the molecule is then magnetically strong field seeking and is lost. To avoid loss, the molecule must switch from the vector sum quantization axis to the vector difference quantization axis, so as to remain magnetically weak field seeking despite the change in relative orientation of the fields. To be more precise, we define the relative orientation of the fields as the sign of $\phi = \vec{E} \cdot \vec{B}$. When ϕ is negative (positive), the trapped state must have the vector difference (sum) quantization axis, so that an increase in magnitude of the magnetic field increases its energy. Orientation changes whenever ϕ changes sign, which occurs in a 2D region given by $\phi = 0$, i.e. $E \perp B$. This region must be 2D, since it is a contour level of the 3D scalar valued function ϕ.

We can quantify this intuitive picture by diagonalizing the molecular Hamiltonian in mixed fields to find the energy splitting between the well trapped substate and its spin-flip partner. The preceding quantization axis discussion suggests that spin-flips occur when crossing the $\phi = 0$ planar region, so we expect to find a correspondingly reduced energy splitting there, since this splitting acts as a barrier to spin-flips. In Fig. 1, the energies of the well trapped state and its spin-flip partner are calculated by diagonalizing OH's $X^2\Pi_{3/2}$ ground state Hamiltonian verses B-field without E-field in panel (a), with fixed E-field and $E \| B$ so that ϕ is maximally nonzero in panel (b), and with fixed E-field and $\phi = 0$ in panel (c). Indeed, we find a striking reduction in energy splitting for a wide range of magnetic fields in panel (c) compared with panel (b). In fact, by series expanding the exact eigenenergies of OH, we find $H_{E\perp B}(B) \approx (\mu_B B)^3 \Delta^2/(d_E E)^4$, Δ the lambda doubling term. The Zeeman splitting is no longer linear, but cubic. This means that the splitting will be small in a much larger region close to $B = 0$ than otherwise.

This observation allows us to develop a scaling law for the loss enhancement in a magnetic quadrupole, oriented with strong axis along $\vec{z}$ as in Fig. 1. For a given trap strength and sample temperature, there is a characteristic energy splitting κ below which spin-flips can occur, calculated from the Landau-Zener formula. In a 2 T/cm gradient with $\mu_B = 1.4$ bohr and $T = 50$mK as for OH in our previous magnetic quadrupole [20], $\kappa = 5$ MHz. As shown in panel (f) of Fig. 1, E-field widens the κ valued energy contour near the trap zero, greatly increasing the flux through this region, which morphs from a small sphere into a broad thin disk. Note also that the energy gradient near the loss region, which also contributes to the Landau-Zener hopping probability, remains nearly identical in the z-direction between panels (e) and (f). This broad thin disk is responsible for the dramatic enhancement of spin-flip loss relative to atoms. We can calculate an enhancement factor simply by comparing the cross sectional area of the disk with that of the original sphere. Solving for B when $H_{E\perp B}(B) = \kappa$ gives the disk radius, so dividing by the $E = 0$ case and squaring gives the flux enhancement factor $\eta = (d_E E/\sqrt{\kappa\Delta})^{8/3}$. Thus E-fields beyond $\sqrt{\kappa\Delta}/d_E$ lead to almost cubic enhancements in spin-flip loss for OH. Rates and enhancements for typical conditions are shown in Table. I. With the electric field used during evaporation for RF knife purposes in [25], spin-flip loss is negligible at 50 mK but relevant at 5 mK. Thus our new understanding will modify the interpretation of the 5 mK endpoint data, but the data still show enhancements in normalized low-field density at 30 mK.

TABLE I. Enhancements and loss rates for OH with typical applied fields. Bold zero field values are equivalent to atom spin-flip loss. E-field required during evaporation and spectroscopy to open avoided crossings for $|e\rangle$ parity states [19, 25]. Background loss is 2 s^{-1}, experiment length 100 ms.

E (V/cm)	45 mK		5 mK		Purpose
	η	$\Gamma\,(s^{-1})$	η	$\Gamma\,(s^{-1})$	
0	1	**0.02**	1	**1.3**	Zero Field
300	5	0.1	9	11	Evaporation
550	17	0.3	40	50	Spectroscopy
3000	1000	19	1600	2000	Polarizing

Generalizing beyond OH, any Hund's case (a) state of any molecule will exhibit a drastically reduced Zeeman splitting near $B = 0$ when $E \perp B$ given by: $H_{E\perp B}(B) \approx (\mu_B B)^{2m_J} \Delta^\alpha/(d_E E)^\beta$, α and β some exponents and m_J the quantum projection number on the total angular momentum J. Thus the order of the dependence of the splitting on magnetic field is not always cubic as for OH's $|f, 3/2\rangle$ state but is given by $2m_J$. Even states with $m_J = 1/2$, which retain a linear Zeeman splitting, are not well trapped for other reasons [23]. This bears out in all test Hamiltonians we have diagonalized, and can be understood intuitively as follows: the Stark effect is blind to the sign of m_J, but still sets the quantization axis for m_J, so that when the magnetic field is orthogonal to the electric, it sees the eigenfunctions it would normally split with linear efficacy as superpositions of $|m_J\rangle \pm |-m_J\rangle$ instead. These superpositions do not shift at all to first order since the linear shift for each component cancels. The magnetic field eventually splits the levels via perturbation of the eigenbasis itself, a task of higher order according to the degree of polarization, i.e. the magnitude of m_J, of the basis state in question.

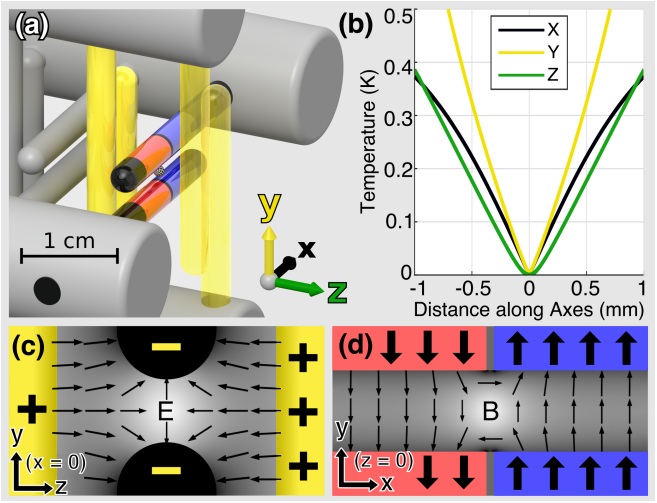

FIG. 2. The last six pins of our Stark decelerator [20] form the trap (a), which is 0.45 mK deep with trap frequency $\nu \approx 4$ kHz (b). Along y the trap is bounded by the 2 mm pin spacing. The yellow pins are positively charged while the central pin pair is grounded, which forms a 2D electric quadrupole trap with zero along the x-axis. This is shown for the $x = 0$ plane (c), with yellow pins artificially projected for clarity since they don't actually intersect the plane. The central pins are magnetized, with two domains each. Blue indicates magnetization along $+\hat{y}$, red along $-\hat{y}$. These domains produce a magnetic quadrupole trap with zero along the z-axis, shown in the $z = 0$ plane (d).

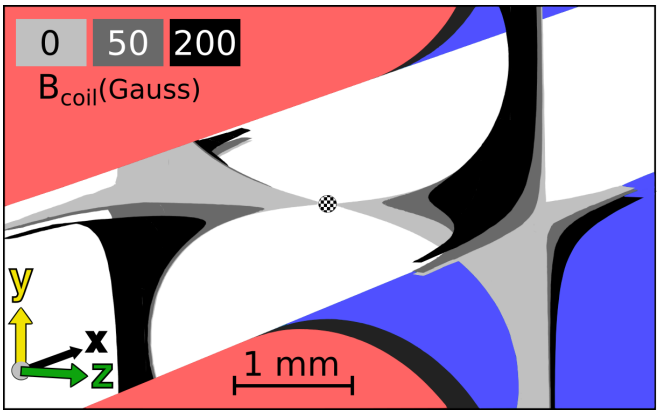

FIG. 3. Surfaces where $E \perp B$ and $\mu_B B/d_E E$ is small enough for spin-flips to occur are shown for three values of B_{coil}. The very center of the trap is indicated; the cloud itself fits within about a 1 mm diameter.

For Hund's case (b) states the rotation of the molecule couples to the electric field, while the electronic orbit and spin separately couple to the magnetic field. To first order the two fields couple different parts of the molecular Hamiltonian and there is not any competition between quantization axes or any spin-flip loss enhancement [24]. However, no molecular state is perfectly Hund's case (b), they always exhibit some degree of spin-rotation coupling, usually denoted by the parameter γ. In the energy regime where γ is large, the molecule is effectively Hund's case (a) and the spin-flip loss reemerges. If κ is much smaller than γ, the spin-flip loss is significantly enhanced. For all laser-cooled molecules and bialkalis thus far, γ is in the tens of MHz [27], and spin-flip loss enhancement is quite significant. Some Hund's case (b) states such as the ground vibrational first rotational state of yttrium oxide (YO) exhibit a protected substate that is magnetically trappable and spin-flip immune [**?**]. This state avoids spin-flips by having $m_F = 0$ in the large γ regime, where F is the total angular momentum including nuclear spin playing the role that J did in our previous explanations. It has no spin-flip partner since $-m_F = m_F$, but is still separated above other states due to the fermi contact interaction.

We can generalize to arbitrary geometries and consider methods to avoid the loss using a simple strategy: avoid $\mu_B B < d_E E$ where $E \perp B$. One way to achieve this is to trap with E-field and superpose B-field. The lambda doublet prevents flips in this configuration, but it correspondingly rounds the trap minimum, weakening confinement. Another option is to trap with both fields and keep zeros overlapped. This was once realized for OH with a superposed magnetic quadrupole and electric hexapole [28]. Such a scheme prevents spin-flip loss enhancement, but does not remove it entirely. It is also susceptible to misalignment induced loss enhancement. A final possibility is to use one field only. While this avoids spin-flip loss enhancement, any experiment which aims to make use of the doubly dipolar nature of molecules cannot accept this compromise.

We opt for a geometry that is distinct from these options: a pair of 2D quadrupole traps, one magnetic and the other electric, with orthogonal centerlines. We achieve these fields in a geometry that matches our Stark decelerator [12], as shown in Fig. 2. This approach is similar to the Ioffe-Pritchard strategy [29], where a 2D magnetic quadrupole is combined with an axial magnetic dipole trap. While this successfully prevents spin-flip loss, axial and radial trapping interfere, resulting in significantly lower trap depths than the 3D quadrupole. We thwart this interference by using electric field for the third direction. Our geometry has $E \perp B$ along both the xz and yz planes, with $\mu_B B < d_E E$ in a large cylinder surrounding the z-axis. However, by adding magnetic field $\vec{B} = B_{\text{coil}}\hat{z}$ along the centerline of the magnetic quadrupole with an external bias coil, a fully tunable scenario emerges.

Adding B_{coil} only slightly rounds the magnetic trapping potential, but it morphs the $E \perp B$ surface from a pair of planes into a hyperbolic sheet, pushing it away from the z-axis where the magnetic field is smallest. This means that small magnitudes of B_{coil} are sufficient to avoid $\mu_B B < d_E E$ where $E \perp B$. In Fig. 3, the surfaces where $E \perp B$ for several B_{coil} magnitudes are shown wher-

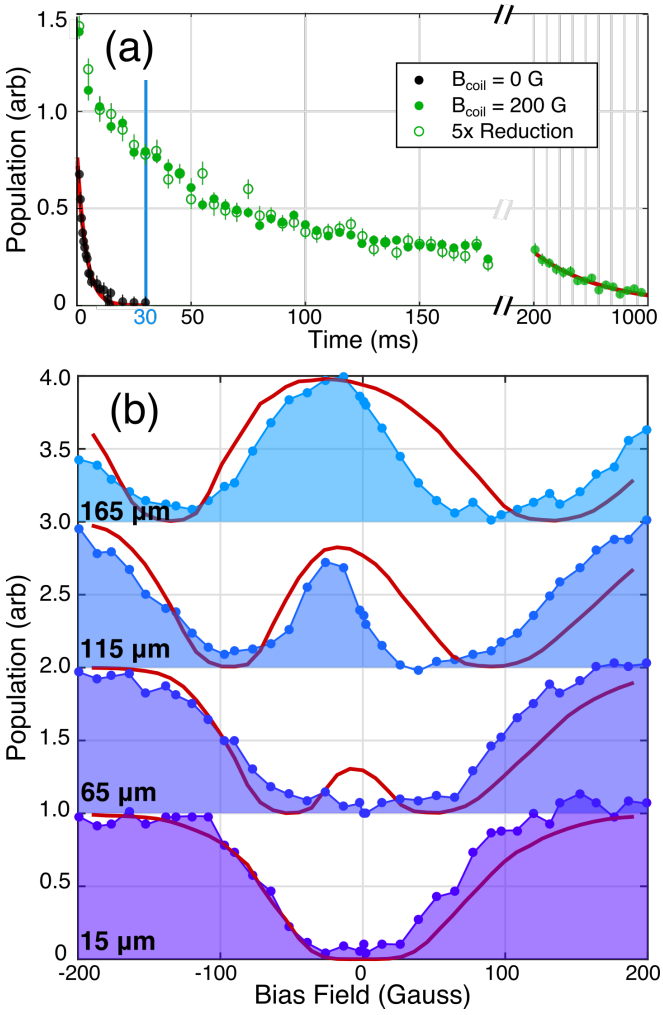

FIG. 4. Time traces (a) without bias field (black), with bias field (green dots), and with modulated density (green circles). One body fits (red) give loss rates of 200 s^{-1} without bias field and 2 s^{-1} with full bias field at long times, in agreement with our background gas pressure. At the fixed time 30ms, population is shown as a function of both pin translation and bias field (b), for several values of pin translation, labeled relative to perfect alignment.

ever the splitting is below the hopping threshold κ. Note how the loss regions are always visible, but they are tuned so far away from the trap center that molecules accessing them have already escaped the trap. The striking difference in molecule trap lifetime with and without B_{coil} can be seen in Fig. 4(a).

As a further confirmation of our $E \perp B$ and $\mu_B B < d_E E$ model of the loss, we translate our magnetic pins along the $\hat{x}$ direction in their mounts to alter the surface where $E \perp B$ and compare experimental data against our expectations. The data are shown in Fig. 4, panel (b). Qualitatively, this translation serves to disrupt the otherwise perfectly 2D magnetic quadrupole by adding a small trapping field $\vec{B} \propto B' z \hat{z}$ along the z-axis. This

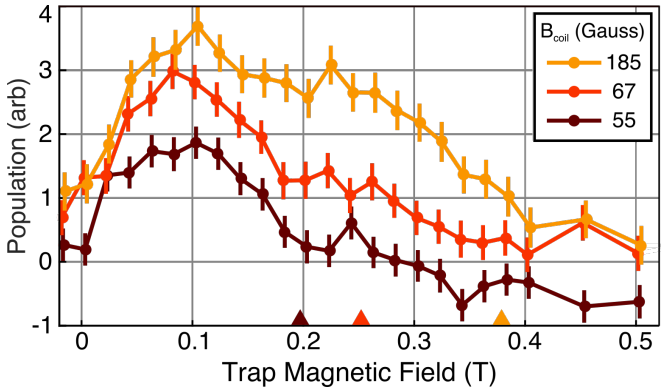

FIG. 5. Microwave spectroscopy at different values of B_{coil}. Increasing B_{coil} increases population and shifts the distribution toward higher fields. Triangles indicate the field at which a molecule can access loss regions for a given B_{coil}.

means that B_{coil} no longer directly tunes the magnetic field magnitude along the z-axis. Instead, B_{coil} must first overcome the slight trapping field along the z-axis, translating a point of zero field along the z axis and eventually out of the trap. The point of zero magnetic field has $\mu_B B < d_E E$ and lies on the $\phi = \vec{E} \cdot \vec{B} = 0$ surface by definition, leading to strong loss unless it is aligned with the trap center, where E is also zero. This means that without any bias field, the loss should actually be a local minimum; as the field is increased in either direction the loss should first worsen and then improve when the zero leaves the trap. This qualitative explanation correctly predicts the observed double well structure in population verses B_{coil}.

Quantitatively, we fit the family of curves shown in Fig. 4(b) by performing an integration of molecule flux weighted by Landau-Zener probability and Maxwell-Boltzmann population over the contorted surfaces where $E \perp B$ for each B_{coil} and pin translation. The computation is performed in COMSOL, with cloud temperature as the only free parameter [26]. The asymmetry of the curves about $B_{\text{coil}} = 0$ comes from a slight shift of the electric quadrupole field caused by an intentional bending of the last pin pair. This bend enhances laser induced fluorescence collection, our detection technique. The fitted temperature is in the $100 - 200$ mK range, larger than expected from our simulations, which already account for known losses [31]. This may be related to microdischarges on the surfaces of the magnetic pins during the final deceleration pulse, since these specially manufactured pins are more difficult to polish. Various more advanced polishing strategies could overcome this limitation.

We further confirm the consistency of our model of the loss using microwave spectroscopy, see Fig. 5. The spectroscopy is performed as in our previous work [25], but with a microwave probe directly exciting free space

modes of our vacuum chamber instead of a bias tee. It is seen that increasing B_{coil} increases population first at low fields and then at higher fields. This is consistent with our calculations of the location of the loss as presented in Fig. 3. In order to perform this spectroscopy, the trapping electric fields are switched off immediately prior to Zeeman specific microwave transfer pulses. Thus the results reflect the Zeeman potential energy only, which is related to the total potential energy in a complex way depending on the Stark energy and $E \perp B$ at a given molecule location. Nonetheless, in the ensemble average the Zeeman and total potential energies should track one another, and the observed shift in population center is clear and in agreement with our expectation.

In the case of lowest applied magnetic field in Fig. 5, a negative going signal is observed. This indicates a build-up in an opposite parity state. Although the spin-flips we have discussed connect $|f, 3/2\rangle$ to $|f, -3/2\rangle$, the latter experiences various avoided crossings at nonzero B-field and E-field. This results in the spin-flipped molecules remaining weakly trapped in a secondary state whose field-dressed state character is of mixed parity or even nearly pure $|e, 3/2\rangle$ strong-field seeking parity in some regions.

With loss removed, we observe a population dependent decay trend (Fig. 4(a), green dots), suggestive of collisions. To test this, we implement a five-fold reduction in initial population and scale the resulting trend by five (green circles). If collisions had contributed, this new trend would decay less rapidly, but we observe no significant change. Our population reduction is achieved early during deceleration, with a microwave field that weakly couples opposite parities and gives the molecules a probability of becoming strong-field seeking and lost from the decelerator. There is no clear reason for this technique to favor molecules that would end up in one part of the eventually trapped phase-space over another, and so the population distribution should be perturbed in no other way than an overall scaling. If there were such a perturbation, it would be surprising for it to precisely counteract a collision-related reduction in decay trend and lead to the observed overlap. An alternative hypothesis for the decay trend is the existence of chaotic trap orbits with long escape times, as seen in other exotically shaped trapping potentials [32].

This absence of a collisional effect contrasts with our earlier evaporation work [25], which as we have mentioned still shows an increase in normalized molecule density at low fields for light cuts from 45 to 30 mK where spin-flip loss is still insignificant. This could be attributable to various differences- a warmer initial temperature, reduced molecule number, or different trap geometry and trap loading process. It is also possible that the spin-flip loss is playing a role at even higher temperatures than we calculate, and that some process we don't yet understand masquerades as a normalized low field density enhancement at 30 mK. The ideal way to resolve any remaining questions would be to continue with the spin-flip loss removed and increase the density as much as necessary to reattain the collisional regime. With this in mind, we have several density-enhancing measures in progress [].

Molecule enhanced spin-flip loss arises in mixed electric and magnetic fields due to a competition between field quantization axes where $E \perp B$ and $\mu_B B < d_E E$. We conclusively demonstrate this effect and overcome it using our dual magnetic and electric quadrupole trap. Our explanation of the effect provides detailed predictions of how its location and magnitude ought to scale with bias field and trap alignment, which we experimentally verify. Our results correct existing predictions about molecular spin-flips in mixed fields and pave the way toward further improvements in molecule trapping and cooling.

We acknowledge the Gordon and Betty Moore Foundation, the ARO-MURI, JILA PFC, and NIST for their financial support. T.L. acknowledges support from the Alexander von Humboldt Foundation through a Feodor Lynen Fellowship. We thank J.L. Bohn and S.Y.T. van de Meerakker for helpful discussions. We thank Goulven Quéméner for his continued involvement in this research.

D.R. and H.W. contributed equally.

* dave.reens@colorado.edu

† Present Address: 5. Physikalisches Institut and Center for Integrated Quantum Science and Technology (IQST), Universität Stuttgart, Pfaffenwaldring 57, 70569 Stuttgart, Germany

[1] L. D. Carr, D. DeMille, R. V. Krems, and J. Ye, New Journal of Physics **11**, 055049 (2009).

[2] S. A. Moses, J. P. Covey, M. T. Miecnikowski, B. Yan, B. Gadway, J. Ye, and D. S. Jin, Science **350**, 659 (2015).

[3] T. Takekoshi, L. Reichsöllner, A. Schindewolf, J. M. Hutson, C. R. Le Sueur, O. Dulieu, F. Ferlaino, R. Grimm, and H.-C. Nägerl, Physical Review Letters **113**, 205301 (2014).

[4] J. W. Park, S. A. Will, and M. W. Zwierlein, Physical Review Letters **114**, 205302 (2015).

[5] M. T. Hummon, M. Yeo, B. K. Stuhl, A. L. Collopy, Y. Xia, and J. Ye, Physical Review Letters **110**, 143001 (2013).

[6] J. F. Barry, D. J. McCarron, E. B. Norrgard, M. H. Steinecker, and D. DeMille, Nature **512**, 286 (2014).

[7] V. Zhelyazkova, A. Cournol, T. E. Wall, A. Matsushima, J. J. Hudson, E. A. Hinds, M. R. Tarbutt, and B. E. Sauer, Physical Review A **89**, 053416 (2014).

[8] M. H. Steinecker, D. J. McCarron, Y. Zhu, and D. DeMille, ChemPhysChem **17**, 3664 (2016).

[9] B. Hemmerling, E. Chae, A. Ravi, L. Anderegg, G. K. Drayna, N. R. Hutzler, A. L. Collopy, J. Ye, W. Ketterle, and J. M. Doyle, Journal of Physics B: Atomic, Molecular and Optical Physics **49**, 174001 (2016).

[10] J. M. Doyle, J. D. Weinstein, R. DeCarvalho, T. Guillet, and B. Friedrich, Nature **395**, 148 (1998).

[11] H. L. Bethlem, G. Berden, and G. Meijer, Physical Review Letters **83**, 1558 (1999).
[12] J. R. Bochinski, E. R. Hudson, H. J. Lewandowski, G. Meijer, and J. Ye, Physical Review Letters **91**, 243001 (2003).
[13] E. Narevicius, A. Libson, C. G. Parthey, I. Chavez, J. Narevicius, U. Even, and M. G. Raizen, Physical Review Letters **100**, 093003 (2008).
[14] A. Wiederkehr, H. Schmutz, M. Motsch, and F. Merkt, Molecular Physics **110**, 1807 (2012).
[15] A. Prehn, M. Ibrügger, R. Glöckner, G. Rempe, and M. Zeppenfeld, Physical Review Letters **116**, 063005 (2016).
[16] A. L. Migdall, J. V. Prodan, W. D. Phillips, T. H. Bergeman, and H. J. Metcalf, Physical Review Letters **54**, 2596 (1985).
[17] W. Petrich, M. H. Anderson, J. R. Ensher, and E. A. Cornell, Physical Review Letters **74**, 3352 (1995).
[18] K. B. Davis, M. O. Mewes, M. R. Andrews, N. J. van Druten, D. S. Durfee, D. M. Kurn, and W. Ketterle, Physical Review Letters **75**, 3969 (1995).
[19] B. K. Stuhl, M. Yeo, B. C. Sawyer, M. T. Hummon, and J. Ye, Physical Review A **85**, 033427 (2012).
[20] B. C. Sawyer, B. K. Stuhl, D. Wang, M. Yeo, and J. Ye, Physical Review Letters **101**, 203203 (2008).
[21] B. K. Stuhl, M. Yeo, M. T. Hummon, and J. Ye, Molecular Physics **111**, 1798 (2013).
[22] M. Lara, B. L. Lev, and J. L. Bohn, Physical Review A **78**, 033433 (2008).
[23] Although the underestimate was only by a factor of three, it is unclear how much of the collisional effect described in [21] remains. This will be the subject of further investigation.
[24] J. L. Bohn and G. Quéméner, Molecular Physics **111**, 1931 (2013).
[25] B. K. Stuhl, M. T. Hummon, M. Yeo, G. Quéméner, J. L. Bohn, and J. Ye, Nature **492**, 396 (2012).
[26] Spin-flip loss would have interfered with evaporation before 5 mK was attained. Some phase space compression does seem to have occurred at 20 mK.
[27] G. Quéméner and J. L. Bohn, Physical Review A - Atomic, Molecular, and Optical Physics **93**, 1 (2016).
[28] B. C. Sawyer, B. L. Lev, E. R. Hudson, B. K. Stuhl, M. Lara, J. L. Bohn, and J. Ye, Physical Review Letters **98**, 1 (2007).
[29] D. E. Pritchard, Physical Review Letters **51**, 1336 (1983).
[30] Soure code: https://github.com/dreens/spin-flip-integration/.
[31] B. C. Sawyer, B. K. Stuhl, B. L. Lev, J. Ye, and E. R. Hudson, European Physical Journal D **48**, 197 (2008).
[32] R. González-Férez, M. Iñarrea, J. P. Salas, and P. Schmelcher, Physical Review E **90**, 062919 (2014).